Check for updates

TRR
JOURNAL OF THE TRANSPORTATION RESEARCH BOARD

Freight Focus

Transportation Research Record
2023, Vol. 2677(2) 98–114
© National Academy of Sciences:
Transportation Research Board 2022
Article reuse guidelines:
sagepub.com/journals-permissions
DOI: 10.1177/03611981221087240
journals.sagepub.com/home/trr
SAGE

Robust Multi-Period Maximum Coverage Drone Facility Location Problem Considering Coverage Reliability

Darshan Rajesh Chauhan[1], Avinash Unnikrishnan[1], Miguel A. Figliozzi[1], and Stephen D. Boyles[2]

Abstract

This study proposes a multi-period facility location formulation to maximize coverage while meeting a coverage reliability constraint. The coverage reliability constraint is a chance constraint limiting the probability of failure to maintain the desired service standard, commonly followed by emergency medical services and fire departments. Further, uncertainties in the failure probabilities are incorporated by utilizing robust optimization using polyhedral uncertainty sets, which results in a compact mixed-integer linear program. A case study in the Portland, OR metropolitan area is analyzed for employing unmanned aerial vehicles (UAVs) or drones to deliver defibrillators in the region to combat out-of-hospital cardiac arrests. In the context of this study, multiple periods represent periods with different wind speed and direction distributions. The results show that extending to a multi-period formulation, rather than using average information in a single period, is particularly beneficial when either response time is short or uncertainty in failure probabilities is not accounted for. Accounting for uncertainty in decision-making improves coverage significantly while also reducing variability in simulated coverage, especially when response times are longer. Going from a single-period deterministic formulation to a multi-period robust formulation boosts the simulated coverage values by 57%, on average. The effect of considering a distance-based equity metric in decision-making is also explored.

Keywords

maximum coverage, facility location, robust optimization, chance constraint, drone, UAV, emergency

Public service agencies like hospitals, fire, rescue, and police departments are required to maintain high levels of service. For example, fire-related incidents require 90% reliability for a 4 min response time (*1*). Similarly, in the case of emergency medical services, the U.S. Emergency Medical Services Act of 1997 requires a 95% response rate within 10 min (*2*). In the United Kingdom, the National Health Service aims to serve 75% and 95% of demands in 8 and 14 min, respectively (*3*). As transportation systems are dynamic and stochastic, an inherent uncertainty in travel time is present. This uncertainty in travel time leads to uncertainty in facility or demand coverage.

Drone or unmanned aerial vehicle (UAV) deliveries are being explored as a quicker, more cost-effective, and more reliable alternative for time-sensitive medical deliveries, emergency scenarios, humanitarian logistics, and other agricultural, security, and military applications (*4, 5*). Large corporations such as Amazon have secured operational licenses and begun field trials (*6*). In addition, there is support from federal programs, such as the Federal Aviation Authority's UAS-BEYOND program (*7*), to test medical applications including delivery of automatic external defibrillators (AEDs), medical prescriptions, and medical emergency response. These

[1]Department of Civil and Environmental Engineering, Portland State University, Portland, OR
[2]Department of Civil, Architectural, and Environmental Engineering, The University of Texas at Austin, Austin, TX

Corresponding Author:
Darshan Rajesh Chauhan, drc9@pdx.edu

medical applications are being field tested in the states of Nevada, North Carolina, and North Dakota, respectively.

Drones have some advantages when compared with traditional ground transportation modes. They can arrive faster by taking more direct paths and avoiding ground-based obstructions or congestion. For ground vehicles, congestion and associated delays are key sources of travel time uncertainty. For drone deliveries, however, uncertainties arise because of weather conditions, mainly from uncertainty about wind speed and direction (*8*).

The effect of stochasticity in environmental factors on the performance of emergency departments is hard to quantify exactly, in addition to being data-intensive. However, reliable estimates for expected values (e.g., mean and variance) and extrema (e.g., minimum and maximum) are much easier to obtain. This is much more true for strategic decisions like facility location when the planning periods are longer. Robust optimization (RO) is a distribution-free approach that allows for incorporating stochasticity with limited information using uncertainty sets. The splitting of a planning period into multiple smaller periods would disaggregate uncertainties and possibly aid RO in tackling them.

This paper considers a robust multi-period maximum coverage facility location problem considering coverage reliability (MP-R) to improve decision-making. The coverage reliability constraints are captured using the chance constraints which provide probabilistic constraint satisfaction guarantee. The final model is developed by integrating the chance constrained approach with robust optimization, similar to Lutter et al. (*2*), and expanded to multiple time periods. The contributions of this paper are:

- Developing a compact mixed-integer linear programming formulation for MP-R using polyhedral uncertainty sets (*9*).
- Developing a case study in the Portland, OR metropolitan area to locate drone launch sites to deliver defibrillators, considering uncertainty in travel times arising from variation in wind speeds and directions.
- Analyzing the value of adding robustness and multiple time periods using a novel Monte Carlo simulation scheme.

A brief literature review is presented in the next section, followed by the development of the mathematical model. The case study is developed and the computational analyses are discussed. Finally, the paper ends with brief conclusions and recommendations for future research.

Literature Review

A plethora of research has already been conducted in the field of emergency medical response. The vast majority of research has been focused around using ground vehicles (i.e., traditional ambulances) for optimizing coverage (*10–13*), survival rates (*14, 15*), amount of relocation (*10, 13, 16*), and crew shifts (*11*). Detailed literature reviews on ambulance location can be found in Aringhieri et al. (*17*), Başar et al. (*18*), and Li et al. (*19*). Recently, there has been increasing interest in the usage of air-based vehicles for emergency medical operations: AED-enabled drones for out-of-hospital cardiac arrests (*20, 21*), drones supplying emergency relief packages (*22, 23*), helicopters (*24*), and air ambulances (*25*). This study focuses on locating AED-enabled drones for tackling out-of-hospital cardiac events in a planning region using a multi-period facility location formulation incorporating reliability in coverage.

Multi-period variants of traditional facility location problems have been studied for various contexts since the seminal work of Ballou (*26*). Nickel and Saldanha da Gama (*27*) provide a review of multi-period facility location problems (MPFLP), and Vatsa and Jayaswal (*28*) provide a brief review of studies considering uncertainties in MPFLP literature. Vatsa and Jayaswal (*28*) note that while demand and cost uncertainties are widely tackled in the MPFLP literature, research tackling supply-side uncertainties (e.g., coverage capabilities) is relatively scarce. Kim et al. (*29*) propose a MPFLP with drones considering uncertainty in flight distances. The study assumes that the probability of a drone's successful return to the launch station is not time-period dependent and that the time periods are long enough that all drone trips are completed within a time period. Ghelichi et al. (*30*) propose a multi-stop drone location and scheduling problem for medical supply delivery. The study assumes deterministic travel speed for drones (i.e., ignoring weather conditions) in multiple periods, and time periods are short and a drone trip is assumed to last over multiple time periods. This study assumes that the probability of timely arrival at a demand location from a launch site is dependent on the time period, and that the time periods are long enough that each drone trip can be completed in a time period.

Erdoğan et al. (*11*) state that appropriately defining coverage and incorporating uncertainty in travel times are the most important considerations in ambulance location. This study defines coverage based on the importance of covering the demand point. Therefore, the coverage importance metric can be a function of various population parameters like size and demographics, and other characteristics like history of emergency requests and equity considerations. Additionally, in most regions, the emergency response systems are required to maintain

adequate service standards. The service standard reliability constraint is modeled as a chance constraint on the probability of timely arrival for each demand point. Therefore, a demand point is considered covered only if the service standard reliability requirements are met for all time periods of the planning period.

The probability of timely arrival at a demand point is linked to the uncertainty in drone travel times which stems from variations in wind speed and direction. Given their dependency on environmental factors, the estimated values of probabilities of timely arrival are not deterministic, but rather uncertain. Tackling parameter uncertainty has been a focus of the mathematical programming community for a long time. Two major approaches exist for tackling uncertainty: stochastic optimization (SO) and robust optimization (RO). SO assumes that a probability distribution of the uncertainty is available, whereas RO assumes no underlying distribution of the uncertainty and considers it to be deterministic and set-based (*31, 32*). A set-based uncertainty structure of RO leads to better computational tractability than SO (*32*). RO immunizes the solution from any manifestation of uncertainty in the described uncertainty set. In general, the larger the size of the uncertainty set, the lower is the objective value (considering maximization objective) and the lower is the probability of constraint violation (*32*). This trade-off between expected objective values and constraint violation can be controlled by varying the size of the uncertainty set. Here, RO using polyhedral uncertainty sets (*9*) is used to tackle uncertainty while maintaining computational tractability. This approach ensures that the robust counterpart of the linear optimization problem is also linear. The interested reader is referred to Ben-Tal et al. (*31*), Bertsimas et al. (*32*), Gabrel et al. (*33*), Gorisson et al. (*34*), Goh and Sim (*35*), and Delage and Ye (*36*) for a more comprehensive picture of RO.

Problem Description

This section first describes the modeling of the coverage reliability constraint and its assumptions. A deterministic multi-period maximum coverage facility location problem with coverage reliability (abbreviated as MP-D) is then formulated. Finally, a robust formulation of MP-D (abbreviated as MP-R) is provided which accounts for uncertainty in the values of coverage failure probabilities.

Consider a set of demand points (represented as I) each with coverage importance c_i, a set of facilities (represented as J), and a set of all time periods (represented as T). Let A be a $|I| \times |J|$ 1–0 accessibility matrix describing if the demand point i can be covered by a facility j. a_{ij}^t is used to represent the probabilistic nature of the (i,j) element of A in time period $t \in T$, while A_{ij} is used for the deterministic initial state of (i,j) element of the matrix A. More specifically, if $A_{ij} = 1$, then $a_{ij}^t = 1$ with probability $(1 - p_{ij}^t)$, and $a_{ij}^t = 0$ with probability p_{ij}^t. If $A_{ij} = 0$, then $a_{ij}^t = 0$ always. Let $\bar{p}_{ij}^t$ be the estimate of p_{ij}^t. The service reliability requirement of achieving a service standard α can then be stated as

$$Pr\left[\sum_{j \in S_i} a_{ij}^t \geq 1\right] \geq \alpha, \tag{1}$$

where $S_i = \{j \in J \,|\, A_{ij} = 1\}$. The above equation potentially considers all the facilities that can access demand point $i \in I$. As a consequence, it is assumed that all the accessible facilities respond to the demand at location i. Under the assumption of independence among the values in A, Equation 1 can be modified as

$$Pr\left[\sum_{j \in S_i} a_{ij}^t \geq 1\right] = 1 - \prod_{j \in S_i} p_{ij}^t \equiv 1 - \prod_{j \in S_i} \bar{p}_{ij}^t \geq \alpha \tag{2}$$

For the above discussion, it is assumed that $\bar{p}_{ij}^t$ completely describes the distribution of variables a_{ij}^t. However, there are errors endemic to sampling (environmental factors) and measurement when estimating the value of p_{ij}^t. Therefore, the values of p_{ij}^t may not be known with complete certainty. This issue is tackled while formulating the MP-R model.

For MP-D and MP-R, the decision-making agency wishes to locate a maximum of q facilities in each time period to maximize the cumulative coverage importance achieved subject to coverage requirements described. Additionally, opened facility locations can be shifted between time periods subject to a facility relocation cost budget constraint.

Deterministic Formulation

Objective:

$$\max_{x,y,z} \quad \sum_{i \in I} c_i x_i \tag{3}$$

Subject to:

$$\prod_{j \in S_i} (\bar{p}_{ij}^t)^{y_j^t} \leq (1 - \alpha)^{x_i} \quad \forall\, i \in I, t \in T \tag{4}$$

$$\sum_{j \in J} y_j^t \leq q \quad \forall\, t \in T \tag{5}$$

$$\sum_{t \in T \setminus \{1\}} \sum_{j \in J} \sum_{k \in J} f_{jk}^t z_{jk}^t \leq B \tag{6}$$

$$\sum_{k \in J} z_{jk}^t = y_j^{t-1} \quad \forall\, j \in J, t \in T \setminus \{1\} \tag{7}$$

Nomenclature

Sets and Indices	
I	Set of all demand points ($i \in I$)
J	Set of all candidate facility locations ($j, k \in J$)
T	Set of all time periods ($t \in T: = \{1, 2, \ldots, \lvert T \rvert\}$)
Parameters	
c_i	Coverage importance of demand point $i \in I$; $c_i \geqslant 0$
A_{ij}	1, if the demand point $i \in I$ can be covered by facility $j \in J$, and 0, otherwise
S_i	Set of facilities $j \in J$ that can cover the demand point $i \in I$; $S_i = \{j \in J \lvert A_{ij} = 1\} \; \forall \, i \in I$
$\bar{p}_{ij}^t$	Nominal probability of failure of covering demand point $i \in I$ by facility $j \in J$ in time period $t \in T$; $0 < p_{ij}^t \leqslant 1$
$\hat{p}_{ij}^t$	Maximum deviation from nominal probability of failure of covering demand point $i \in I$ by facility $j \in J$ in time period $t \in T$; $0 \leqslant \hat{p}_{ij}^t < p_{ij}^t + \hat{p}_{ij}^t \leqslant 1$
q	Maximum number of facilities that can be located; $q \in \mathbb{Z}^+ \cup \{0\}$
α	Required coverage threshold; $0 \leqslant \alpha \leqslant 1$
Γ_i^t	Maximum number of delivery paths to demand point i that can achieve worst-case probability of failure simultaneously in time period $t \in T$; $\Gamma_i^t \in \mathbb{Z}^+ \cup \{0\}$
f_{jk}^t	Cost associated with shifting the facility from location $j \in J$ to location $k \in J$ at the beginning of time period $t \in T$
B	Facility shifting cost budget
Decision Variables	
x_i	1, if demand location $i \in I$ is covered with given coverage threshold; 0, otherwise
y_j^t	1, if candidate facility location $j \in J$ is open during time period $t \in T$; and 0, otherwise
z_{jk}^t	1, if a facility is moved from location $j \in J$ to location $k \in J$ at the beginning of time period $t \in T \backslash \{1\}$; and 0, otherwise

$$\sum_{j \in J} z_{jk}^t = y_k^t \quad \forall \, k \in J, t \in T \backslash \{1\} \tag{8}$$

$$x_i \in \{0, 1\} \quad \forall \, i \in I \tag{9}$$

$$y_j^t \in \{0, 1\} \quad \forall \, j \in J, t \in T \tag{10}$$

$$z_{jk}^t \in \{0, 1\} \quad \forall \, j, k \in J, t \in T \backslash \{1\} \tag{11}$$

For the deterministic formulation, it is assumed that $p_{ij}^t = \bar{p}_{ij}^t$. Equation 3 represents maximizing coverage importance. In Equation 4, the demand point $i \in I$ is covered only if the probability of failure to cover it is less than $(1 - \alpha)$ for all time periods $t \in T$. Note that all accessible open facilities respond to meet the demand at point $i \in I$. Equation 5 enforces that no more than q facilities can be opened.

Equation 6 is a generalized cost constraint relating to the shifting facility locations. Equations 7 and 8 are transportation allocation constraints. Note that using $f_{jj}^t = 0$ for all $j \in J, t \in T \backslash \{1\}$, and 1, otherwise, would limit the total number of facility location shifts to B. Equations 9 to 11 are variable definitions. However, the formulation is not linear because of Equation 4. Applying logarithm function on both sides of Equation 4 yields:

$$\sum_{j \in S_i} w_{ij}^t y_j^t \leqslant \beta x_i \quad \forall \, i \in I, t \in T \tag{12}$$

where w_{ij}^t and β represent $\log(\bar{p}_{ij}^t)$ and $\log(1 - \alpha)$, respectively. The above formulation (Equations 3 and 5–12) is referred to as the deterministic multi-period facility location problem considering coverage reliability, abbreviated as MP-D. MP-D is an integer linear program and can be solved using standard mixed-integer programming (MIP) solvers.

Robust Formulation

The parameter p_{ij}^t represents the probability that the facility $j \in J$, in time period $t \in T$, will fail to cover the demand point $i \in I$ in a given service time threshold τ. However, because of sampling errors stemming from environmental factors like variations in travel times throughout the day, the estimated values of parameters p_{ij}^t are uncertain. Later, in the presented case study of delivering AED-enabled drones, this variation occurs primarily from changing wind speeds and directions. As the complete probability distribution of p_{ij}^t is arduous to obtain in comparison with the bounds of its variation, a robust optimization using polyhedral uncertainty sets is used (*9*) to incorporate this uncertainty. Let $\hat{p}_{ij}^t$ be the maximum deviation of $\bar{p}_{ij}^t$. For the robust model, it is assumed that $p_{ij}^t \in [\bar{p}_{ij}^t - \hat{p}_{ij}^t, \bar{p}_{ij}^t + \hat{p}_{ij}^t]$. Of all the facilities servicing demand point i, up to Γ_i^t facilities observe worst-case failure probabilities (i.e., $p_{ij}^t = \bar{p}_{ij}^t + \hat{p}_{ij}^t$), whereas the rest observe nominal failure probabilities

(i.e., $p_{ij}^t = \bar{p}_{ij}^t$). This allocation happens in such a way that the probability of failing to serve demand point i is maximized.

Objective:

$$\max_{x,y,z} \quad \sum_{i \in I} c_i x_i \tag{13}$$

Subject to:

$$\max_{\{U \subseteq S_i, |U| \leq \Gamma_i\}} \left[\prod_{j \in U} (\bar{p}_{ij}^t + \hat{p}_{ij}^t)^{y_j^t} \prod_{j \in S_i \setminus U} (\bar{p}_{ij}^t)^{y_j^t} \right] \leq (1-\alpha)^{x_i} \quad \forall\, i \in I, t \in T \tag{14}$$

$$\sum_{j \in J} y_j^t \leq q \quad \forall\, t \in T \tag{15}$$

$$\sum_{t \in T \setminus \{1\}} \sum_{j \in J} \sum_{k \in J} f_{jk}^t z_{jk}^t \leq B \tag{16}$$

$$\sum_{k \in J} z_{jk}^t = y_j^{t-1} \quad \forall\, j \in J, t \in T \setminus \{1\} \tag{17}$$

$$\sum_{j \in J} z_{jk}^t = y_k^t \quad \forall\, k \in J, t \in T \setminus \{1\} \tag{18}$$

$$x_i \in \{0,1\} \quad \forall\, i \in I \tag{19}$$

$$y_j^t \in \{0,1\} \quad \forall\, j \in J, t \in T \tag{20}$$

$$z_{jk}^t \in \{0,1\} \quad \forall\, j,k \in J, t \in T \setminus \{1\} \tag{21}$$

Equation 13 represents the maximization of coverage importance. Incorporating uncertainty in the failure probabilities in Equation 4 yields Equation 14. The left-hand side (lhs) of Equation 14 seeks to find the absolute worst-case probability of failure such that at most Γ_i facilities servicing the demand point $i \in I$ can individually observe worst-case failure probability. Demand point $i \in I$ is considered covered only if the lhs of Equation 14 is less than $(1-\alpha)$. Generally, incorporating robustness into a problem imparts conservatism by realizing worst-case objective value subject to certain criteria (*9, 37*). This leads to the robustness sub-problem being in conflict with the overall objective. Here, worst-case realizations of failure probability in Equation 14 reduce the chance of the demand point i being covered, and while the overall objective (Equation 13) wants to increase the chances of demand point i being covered. In other words, the current formulation is a bilevel optimization problem which cannot be solved directly using MIP solvers. Dualizing the robustness sub-problem would overcome this issue and align both objectives correctly, and yield a single level mixed-integer linear problem. Equations 15 to 21 have the same meaning as Equations 5 to 11. Taking the logarithm of Equation 14 yields:

$$\max_{\{U \subseteq S_i, |U| \leq \Gamma_i\}} \Big[\sum_{j \in U} \log(\bar{p}_{ij}^t + \hat{p}_{ij}^t) \cdot y_j^t + \sum_{j \in S_i \setminus U} \log(\bar{p}_{ij}^t) \cdot y_j^t \Big] \leq \log(1-\alpha) \cdot x_i \quad \forall\, i \in I, t \in T \tag{22}$$

Let $\hat{w}_{ij}^t$, w_{ij}^t, and β represent $\log(\bar{p}_{ij}^t + \hat{p}_{ij}^t)$, $\log(\bar{p}_{ij}^t)$, and $\log(1-\alpha)$, respectively. Note that $\hat{w}_{ij}^t \geq w_{ij}^t$. Rewriting $\hat{w}_{ij}^t$ as $w_{ij}^t + (\hat{w}_{ij}^t - w_{ij}^t)$, we re-write Equation 22 as:

$$\sum_{j \in S_i} w_{ij}^t y_j^t + \max_{\{U \subseteq S_i, |U| \leq \Gamma_i\}} \left[\sum_{j \in U} (\hat{w}_{ij}^t - w_{ij}^t) \cdot y_j^t \right] \leq \beta x_i \quad \forall\, i \in I, t \in T \tag{23}$$

The optimization problem described on the lhs of Equation 23 can be written as:

For each $i \in I$, $t \in T$:

$$SP_i^t: \quad \max_{\gamma} \quad \sum_{j \in S_i} w_{ij}^t y_j^t + \sum_{j \in S_i} (\hat{w}_{ij}^t - w_{ij}^t) y_j^t \gamma_{ij}^t \tag{24}$$

$$\sum_{j \in S_i} \gamma_{ij}^t \leq \Gamma_i^t \tag{25}$$

$$\gamma_{ij}^t \in \{0,1\} \quad \forall\, j \in S_i \tag{26}$$

The constraint coefficient matrix of the above sub-problem is totally unimodular, and Γ_i^t are non-negative integer values. Therefore, γ_{ij}^t can be linearized to the interval [0,1] without loss of optimality. Let, θ_i^t and σ_{ij}^t be the dual variables associated with Equation 25 and the upper bound of Equation 26, respectively. Taking the dual of the formulation represented by Equations 24 to 26, yields:

For each $i \in I$, $t \in T$:

$$SPD_i^t: \quad \min_{\sigma,\theta} \quad \sum_{j \in S_i} w_{ij}^t y_j^t + \sum_{j \in S_i} \sigma_{ij}^t + \Gamma_i^t \theta_i^t \tag{27}$$

$$\sigma_{ij}^t + \theta_i^t \geq (\hat{w}_{ij}^t - w_{ij}^t) y_j \quad \forall\, j \in S_i \tag{28}$$

$$\sigma_{ij}^t \geq 0 \quad \forall\, j \in S_i \tag{29}$$

$$\theta_i^t \geq 0 \tag{30}$$

Strong duality, along with the totally unimodular property, ensures that problems SPD_i^t (Equations 27 to 30) and SP_i^t (Equations 24 to 26), and consequently also the lhs of Equation 14, are equivalent. Incorporating SPD_i^t in the Equation 23, updates the robust formulation (Equations 13, 15 to 21, 23) to:

Objective:

$$\max_{x,y,z,\sigma,\theta} \quad \sum_{i \in I} c_i x_i \tag{31}$$

Subject to:

$$\sum_{j\in S_i} w_{ij}^t y_j^t + \sum_{j\in S_i} \sigma_{ij}^t + \Gamma_i^t \theta_i^t \leqslant \beta x_i \quad \forall\, i \in I, t \in T \tag{32}$$

$$\sigma_{ij}^t + \theta_i^t \geqslant (\hat{w}_{ij}^t - w_{ij}^t) y_j^t \quad \forall\, j \in S_i, i \in I, t \in T \tag{33}$$

$$\sum_{j\in J} y_j^t \leqslant q \quad \forall\, t \in T \tag{34}$$

$$\sum_{t\in T\setminus\{1\}} \sum_{j\in J} \sum_{k\in J} f_{jk}^t z_{jk}^t \leqslant B \tag{35}$$

$$\sum_{k\in J} z_{jk}^t = y_j^{t-1} \quad \forall\, j \in J, t \in T\setminus\{1\} \tag{36}$$

$$\sum_{j\in J} z_{jk}^t = y_k^t \quad \forall\, k \in J, t \in T\setminus\{1\} \tag{37}$$

$$x_i \in \{0,1\} \quad \forall\, i \in I \tag{38}$$

$$y_j^t \in \{0,1\} \quad \forall\, j \in J, t \in T \tag{39}$$

$$^{t}_{jk} \in \{0,1\} \quad \forall\, j,k \in J, t \in T\setminus\{1\} \tag{40}$$

$$\sigma_{ij}^t \geqslant 0 \quad \forall\, i \in I, j \in J, t \in T \tag{41}$$

$$\theta_i^t \geqslant 0 \quad \forall\, i \in I, t \in T \tag{42}$$

The above formulation is referred to as the robust maximum coverage facility location problem considering coverage reliability, abbreviated as MP-R. MP-R is a mixed-integer linear program and can be solved using open-source or commercially-available MIP solvers. For cases when $|T|$ is large, the computational times using a MIP solver could be prohibitively large. The authors recommend decomposition-based methodologies for such cases. For example, applying Lagrangian relaxation to Equations 32 and 33 decomposes MP-R into four subproblems, of which three can be trivially solved. The development of computationally-efficient heuristics is left as a future research endeavor.

Computational Analysis

This section first describes the experimental setting of the case study conducted in the Portland, OR metropolitan area. Three types of analysis are then conducted: computational performance, the evaluating the value of considering robustness and multiple periods using a Monte Carlo simulation scheme, and finally, incorporating equity in decision-making.

The feasibility of using UAVs or drones for delivering defibrillators to demand points in the Portland, OR metropolitan area is evaluated here. The Portland Metro service area consists of 122 ZIP Code Tabulation Areas (ZCTA) which act as demand points, and 104 community centers which act as potential launch sites, as detailed in Chauhan et al. (*22*) and shown in Figure 1. Drones are evaluated against two service standards: the National Fire Protection Association's emergency

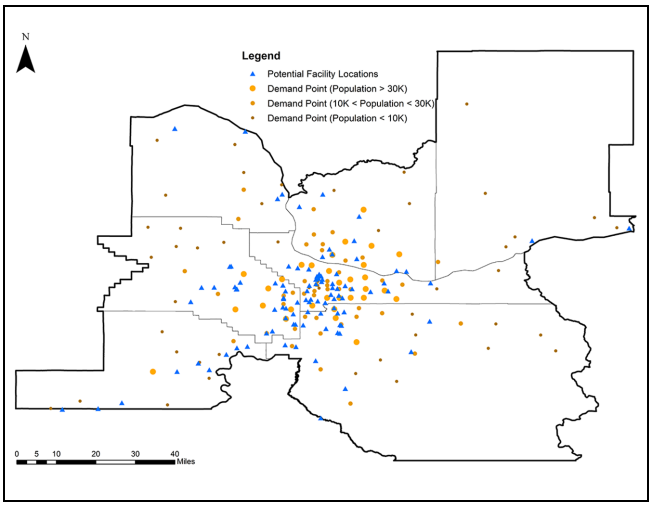


Figure 1. Locations of demand points and facility locations in Portland metropolitan area.

response standard of providing coverage reliability of 90% within in a response time of 4 min (*1*), abbreviated as *SS*1; and, the 1997 U.S. Emergency Medical Services Act service response standard of providing coverage reliability of 95% within a response time of 10 min (*2*), abbreviated as *SS*2. Two service standards are selected to evaluate the effect of increasing response time on system performance and the value of data disaggregation using multiple time periods. All drones are equipped with an AED, each weighing 1.5 kg (*38*). A major factor leading to uncertainty in drone response times is wind speed and direction. The calculation of bounds of probability of failure (lower bound: *p_best*; upper bound: *p_worst*) for delivering from a launch site to a demand point is carried out using a procedure described in Algorithm 1, similar to Glick et al. (*8*), with sample size $n = 10,000$. The upper bound of probability of failure (*p_worst*) is considered as worst-case probability ($\bar{p} + \hat{p}$). The nominal probability of failure ($\bar{p}$) is an average of bounds of variation weighted according to the distribution of wind directions.

A demand point is considered accessible by a launch site if the following two conditions are met. First, the amount of battery power expended to go to the demand point and return is less than the total available battery in the nominal scenario, calculated using the formula provided in Figliozzi (*39*). The total battery capacity of the drone is divided in two parts: total available battery and battery safety factor. As in Chauhan et al. (*22*), it is assumed that drones ignore obstacles in the urban landscape and travel over Euclidean distances, and that the energy consumed in VTOL operations is accommodated in the battery safety factor. Second, the time required to reach the demand point in the most favorable wind

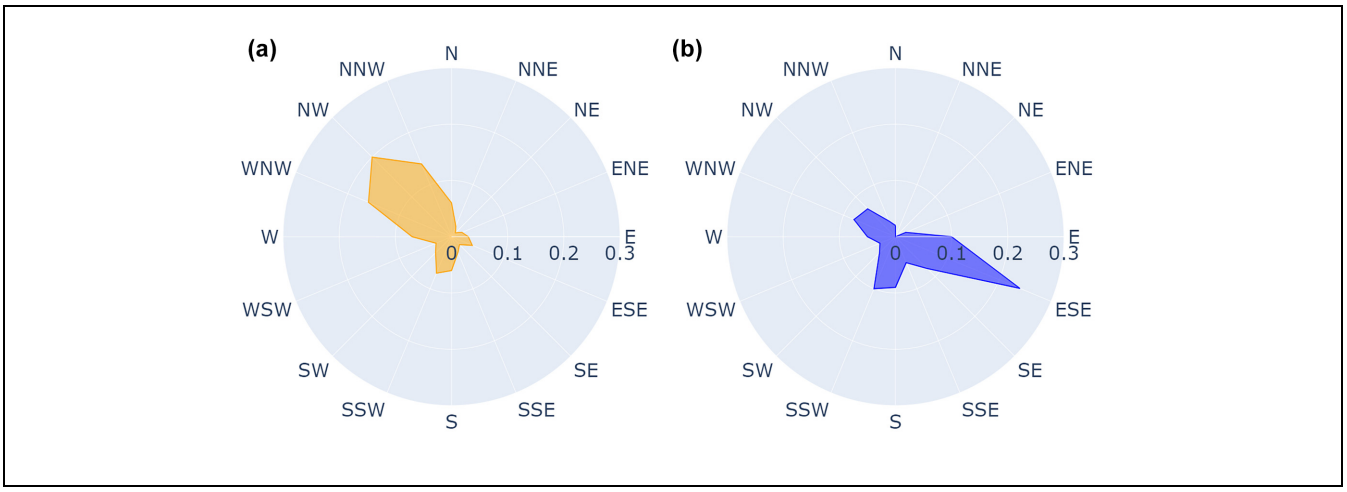


Figure 2. Wind direction distribution in Portland, OR: (*a*) summer and (*b*) winter.

Algorithm 1 Calculating bounds of probability of failure

Input sample size n, wind speed and direction distributions for each time period $t \in T$, maximum possible wind speed (v_wind_max), probability distribution of wind directions, response time (τ), drone travel speed (v_drone), and distance ($dist_act$) and delivery angle from facility j to demand point i.
Calculate $wt[i,j,t]$ which is the probability that the wind direction is not aligned with the delivery direction (i.e., difference is greater than 90°) from facility j to demand point i in time period t using the input information.
for $t \in T$ **do**
  Generate $windspeeds[t]$, an array of size n, following a lognormal distribution with given input parameters and a maximum value of v_wind_max.
  $dist_best = (v_drone + windspeeds[t]) \cdot \tau$
  $dist_worst = (v_drone - windspeeds[t]) \cdot \tau$
  for $i \in I$ **do**
    for $j \in J$ **do**
      $p_best[i,j,t] = \max\{length(where(dist_best < dist_act[i,j])),\ 1\}/n$
      $p_worst[i,j,t] = \max\{length(where(dist_worst < dist_act[i,j])),\ 1\}/n$ $p_nominal[i,j,t] = (1 - wt[i,j,t]) \cdot p_best[i,j,t] + wt[i,j,t] \cdot p_worst[i,j,t]$
    end for
  end for
end for

direction and speed is less than the provided response time. The coverage importance metric is dependent on the normalized population of the demand point. The ZCTA population estimates for the demand points were adopted from 2017 American Community Survey five-year estimates (*40*).

The summary of parameter specifications is provided below (*8, 39*).

- Maximum available battery: 777 Wh
- Battery safety factor: 20% of maximum available battery (Total available battery = maximum available battery − battery safety factor = 621.6 Wh)
- Sum of drone tare and battery mass: 10.1 kg
- Lift-to-drag ratio: 2.8445
- Total power transfer efficiency: 0.66
- Nominal travel speed of drone: 20 meters per second (mps)
- Maximum number of drones serving demand point i in time period t that can achieve worst-case probability of failure (Γ_i^t): 1
- c_i = Normalized population of demand point $i = \left\lceil \frac{100 \times \text{population of demand point } i}{\text{maximum population of demand points}} \right\rceil$ where $\lceil u \rceil$ due represents the ceiling function, that is, the least integer greater than or equal to u.
- Wind speed and direction distributions (see Figure 2) are available openly at https://github.com/drc1807/RMP-MCFLP-CR
- Maximum possible wind speed: 68 mph (30.3987 mps)
- The planning period is one year. In Portland, the wind direction is primarily in the northwest direction in the summer months (April to September), whereas, in the winter months (October to March), the wind primarily blows in the east-southeast direction (see Figure 2). This study investigates the value of using a multi-period formulation with $T = \{\text{Summer}, \text{Winter}\}$ over a single-period formulation with $T = \{\text{WholeYear}\}$.

The model coverage (in %) is given as:

$$\text{Model Coverage} = \frac{\text{Objective Value of Model}}{\sum_{i \in I} c_i} \times 100 \quad (43)$$

The cost of shifting a facility located at $j \in J$ in time period $(t-1)$ to a location $k \in J, k \neq j$ in time period t is considered to be 1, and 0, if the location does not change. Alternatively put, $f_{jj}^t = 0 \, \forall j \in J, t \in T \backslash \{1\}$, and 1, otherwise. This limits the total number of facility location shifts to the facility shifting cost budget B. The default value of B used here is $\lfloor 0.35q \rfloor$, where q is the maximum number of drone launch sites that can be opened.

The experiments are performed on four models: MP-R, MP-D, MP-R with $T = \{\text{WholeYear}\}$ (abbreviated as SP-R), and MP-D with $T = \{\text{WholeYear}\}$ (abbreviated as SP-D) considering a planning period of a whole year. Models are solved using Gurobi optimization (*41*) in Python interface on a Windows 10 desktop with Intel i7-7700K processor and CPU specifications of 3.6 GHz, four cores, eight logical processors, and 32 GB of RAM. Experiments to evaluate the computational efficiency with an increasing number of drone launch sites (q) are conducted, followed by the evaluation of the value added by robustness and granularity of information (through multiple time periods). Additionally, the effect of adding equity in decision-making is explored.

Computational Efficiency

Prohibitive computational times can often be a barrier to the adoption of models in real life. In the present case, the planning period is fairly long (a whole year), and therefore no computational time limit was adopted for Gurobi. All the four models, for both service standards and given default values of parameters, converged in less than 2 h for a range of q values, indicating that the development of time-efficient heuristics was not required. The model coverage values with their computational times are provided in Table 1.

The effect of adding additional time periods is found to be more profound than the effect of adding robustness to the formulation. On average, for SS1, adding robustness increases computational time by 5.2 times, whereas adding additional time period increases computational times by 37.0 times. For SS2, these values are 24.5 times and 49.5 times, respectively. The primary reason behind this is the number of constraints added to the model. A multi-period formulation requires the facility transfer variables z which adds $2 \cdot |J| \cdot |T \backslash \{1\}|$ facility matching equality constraints along with a facility relocation budget constraint. Additionally, $|T| - 1$ simultaneous coverage reliability constraints are also added which further deteriorates computational performance. On the other hand, adding robustness adds more variables and constraints to the model, but the constraints are computationally simpler. The accessibility matrix A is more sparse for the SS1 models than SS2 models, which leads to better computational performance.

The addition of multiple periods to the formulation decreases the model coverage by a little amount (0.8% on average). This is because the satisfaction of multiple coverage reliability constraints is required for demand point coverage. As expected, adding robustness decreases the model coverage by a significant amount (4.9% on average) as a consequence of accounting for worst-case scenarios.

Value of Developing Multi-Period Formulation and Adding Robustness

The value of using more information (through adding robustness and multiple time periods) in a model is evaluated in this section utilizing a Monte Carlo simulation-based (MCS) framework. Generally, adding robustness to a formulation reduces the model coverage but should provide for better real-life performance, thereby reducing the gap between what is expected (model coverage) and what happens (simulated coverage). Similarly, having potentially different facility location layouts in different time periods should boost simulated coverage.

An MCS framework is proposed to quantify the value of using additional information. In an MCS scenario s, the time period is t^s, and $n = 1000$ values of wind directions and speeds are randomly generated. In this case, an MCS scenario $s$can be thought of as a day of the year, and n is the number of wind speed and direction observations made throughout the day. Therefore, for multi-period formulations, t^s = "Summer" with probability $\frac{183}{365}$ and t^s = "Winter" with probability $\frac{182}{365}$. For single-period formulations, t^s = "Whole Year" with probability 1. Depending on the value of t^s, the wind speeds are generated as in Algorithm 1 and wind directions are chosen as per the distributions of the time period. These angles and speeds are combined with the originally projected delivery angles and nominal drone delivery speed to find effective drone speed. The effective drone speeds are then utilized to determine the realizations of the probability of failure for the scenarios ($\tilde{p}^s$).

The solutions obtained from the robust and the deterministic formulations for the variable $y$are denoted by y^*. The new values for the variable x (denoted by $\tilde{x}$) and the actual coverage are calculated using $y^*$and $\tilde{p}^s$. For multi-period formulation, the facility location layout is determined by the simulation time period t^s. A total of 100 MCS scenarios are evaluated and the algorithm for the described MCS is detailed in Algorithm 2.

The simulated coverage values for all four models with default values are presented in Table 2. For SS1 (providing 90% coverage reliability in 4 min), extending to multi-period formulation improves average simulated coverage by 0.29 times on average for robust models, and by 0.41 times on average for deterministic models.

Table 1. Computational Efficiency

Service standard	No. of drone launch sites, q	Model coverage (%)				Computational time (seconds)			
		MP-R	MP-D	SP-R	SP-D	MP-R	MP-D	SP-R	SP-D
SS1	3	12.57	15.76	12.9	15.76	32	6	2	1
	6	24.37	27.41	24.64	28.19	109	15	3	1
	9	33.52	37.93	34.62	38.8	416	17	3	1
	12	41.9	47.02	42.64	48.36	444	33	2	1
	15	49.28	53.9	49.37	55.6	44	23	2	1
	20	55.45	62.31	55.21	62.99	49	8	2	1
	25	59.92	67.19	59.09	67.4	44	4	2	1
	30	62.28	68.36	62.1	68.56	5	4	1	1
	35	62.28	68.5	62.28	68.71	2	1	1	1
SS2	3	35.37	44.85	39.09	46.31	5736	152	38	2
	6	62.69	69.99	64.75	72.53	3937	152	64	1
	9	75.8	82.18	77.26	83.02	1342	26	44	1
	12	82.6	86.23	83.28	87.84	569	40	67	1
	15	87.01	89.6	87.19	90.91	694	44	32	1
	20	90.73	93.38	90.88	93.95	274	108	20	1
	25	92.58	94.73	92.76	95.68	45	48	9	1
	30	93.21	95.23	93.36	96.39	31	2	14	1
	35	93.38	95.29	93.53	96.63	2	1	1	1

Note: MP-R = multi-period robust model; MP-D = multi-period deterministic model; SP-R = single-period robust model; SP-D = single-period deterministic model. SS1 provides 90% coverage reliability in a response time of 4 min. SS2 provides 95% coverage reliability in a response time of 10 min.

Algorithm 2. Monte Carlo simulation for evaluating coverage

Input number of MCS scenarios (*MCS_s*), number of wind speed and direction observations per scenario (n), probability distribution of time periods $t \in T(\pi)$, other model input parameters Solve the model and determine y^*, the optimum values of decision variable y
Determine J_i, the set of open and accessible facilities for each demand point $i \in I$
$s = 1$
$simulated_coverage = zeros(MCS_s)$
while $s \leqslant MCS_s$ **do**
  Randomly select simulation time period t^s, such that $t^s = t$ with probability π_t
  Generate $windspeeds[t^s]$, an array of n elements, as in Algorithm 1
  Generate $windangles[t^s]$, an array of n elements, based on the probability distribution in time period t^s
  Determine effective delivery angles and effective drone speeds using vector algebra.
  For each i, j combination, calculate $dist_cov_{ij}^s$, an array of length n describing distances covered by drones using effective delivery angles and effective drone speeds.
  For each i, j combination, calculate $\tilde{p}_{ij}^s = length(where(dist_cov_{ij}^s < dist_act[i,j]))/n$
  $\tilde{w}^s = \log(\tilde{p}^s)$
  $\tilde{x}^s = zeros(length(I))$
  for $i \in I$ **do**
    if $\sum_{j \in J_i} \tilde{w}_{ij}^s y_j^* \leqslant \beta$ **then**
      $\tilde{x}_i^s = 1$
    end if
  end for
  $simulated_coverage[s] = \frac{\sum_{i \in I} c_i \tilde{x}_i^s}{\sum_{i \in I} c_i} \times 100$
  $s + = 1$
end while

Whereas for SS2 (providing 95% coverage reliability in 10 min), the improvements in average simulated coverage are by 0.02 times for robust models, and by 0.24 times for deterministic models. The improvements are higher when the response time is short because the importance of choosing the right set of facility locations increases. An explanatory factor would be that multi-period formulation allows for more flexibility by allowing changing facility locations for different periods. The extent of facility relocation is depicted in Figure 3. The results reveal that at least 40% of the relocation budget is used when 15 or more facilities are opened. To investigate further the role of facility relocation, consider the visualization of facility location by season for MP-R SS2 model with $q = 15$, as an example, in Figure 4. Based on the wind patterns in Portland (see Figure 2), it is expected that in the summer season the facilities will provide better coverage reliability to demand locations in the west and/or north directions of them. As a result, the facility locations should be skewed a little bit toward the eastern and/or southern region of the operational area. Similarly, the locations in the winter season should be skewed a little bit toward the western and/or northern region. For the example considered, it is indeed noted that the centroid of facility locations opened in summer only is to the east of the centroid of facility locations opened in winter only, which is in agreement with the hypothesis.

For SS1, the improvements in average simulated coverage achieved by adding robustness to multi-period and single-period formulations are by 0.14 times and 0.28

Table 2. Value of Extending to Multi-Period Formulation and Adding Robustness

		SS1				SS2			
			Simulated coverage (%)				Simulated coverage (%)		
Model	No. of drone launch sites, q	Model Cov. (%)	Minimum	Average	Maximum	Model Cov. (%)	Minimum	Average	Maximum
MP-R	3	12.57	5.96	9.28	11.11	35.37	21.42	26.47	32.6
	6	24.37	13.89	16.59	19.55	62.69	36.59	46.01	56.38
	9	33.52	16.3	22.3	26.97	75.8	56.08	63.44	67.07
	12	41.9	24.52	29.96	35.67	82.6	66.18	72.25	79.38
	15	49.28	32.39	37.82	44.85	87.01	72.77	75.36	79.02
	20	55.45	35.58	45.26	53.67	90.73	72.62	78.47	85.97
	25	59.92	43	48.71	54.68	92.58	77.26	81.81	89.09
	30	62.28	48.99	52.58	56.05	93.21	77.98	83.21	88.86
	35	62.28	50.92	53.26	56.53	93.38	86.41	90.91	92.7
MP-D	3	15.76	5.81	8.56	10.25	44.85	23.27	24.75	28.07
	6	27.41	7.9	14.03	19.43	69.99	14.96	31.01	45.74
	9	37.93	14.66	21.79	28.22	82.18	45.05	51.95	60.25
	12	47.02	19.22	27.83	35.43	86.23	47.44	55.65	66.15
	15	53.9	24.76	32.04	39.81	89.6	41.87	51.32	64.99
	20	62.31	25.3	35.16	44.31	93.38	50.48	60.82	71.48
	25	67.19	34.45	40.98	47.5	94.73	68.33	74.49	78.55
	30	68.36	37.22	46.33	55.69	95.23	67.04	77.36	84.77
	35	68.5	40.88	48.01	58.19	95.29	77.83	83.27	90.67
SP-R	3	12.9	1.1	3.54	7.87	39.09	19.34	28.89	32.93
	6	24.64	10.37	11.96	18.06	64.75	36.92	42.25	52.18
	9	34.62	14.36	17.66	24.67	77.26	52.89	62.33	68.47
	12	42.64	23.81	28.73	34.92	83.28	58.88	65.28	74.91
	15	49.37	26.91	34.26	43	87.19	68.98	77.46	83.37
	20	55.21	29.05	40.63	50.63	90.88	70.98	78.71	84.86
	25	59.09	40.05	45.95	53.93	92.76	77.18	80.4	82.93
	30	62.1	42.01	50.33	57.33	93.36	76.28	81.65	89.06
	35	62.28	46.84	52.95	58.94	93.53	87.34	89.74	91.87
SP-D	3	15.76	3.93	4.53	6.23	46.31	18.98	22.57	26.82
	6	28.19	3.72	6.44	9.92	72.53	22.56	29.9	37.4
	9	38.8	7	11.68	16.78	83.02	32.06	41.54	47.94
	12	48.36	14.75	22.49	31.35	87.84	30.78	38.76	44.73
	15	55.6	19.19	25.42	32.75	90.91	29.14	38.72	46.28
	20	62.99	21.22	29.61	38.53	93.95	30.13	40.03	48.81
	25	67.4	32.03	40.82	47.94	95.68	54.02	57.29	63.29
	30	68.56	33.97	42.47	50.83	96.39	61.29	67.56	74.76
	35	68.71	39.6	48.4	54.08	96.63	72.82	77.38	80.39

Note: MP-R = multi-period robust model; MP-D = multi-period deterministic model; SP-R = single-period robust model; SP-D = single-period deterministic model; Cov. = Coverage. SS1 provides 90% coverage reliability in a response time of 4 min. SS2 provides 95% coverage reliability in a response time of 10 min.

times, respectively. For SS2, the improvements in average simulated coverage are by 0.23 times and 0.51 times for multi-period and single-period formulations, respectively. The improvement by adding robustness to a multi-period formulation is lower as more detailed information has been accounted which leads to lower variability in data in each time period. Similarly, the variability in distance traveled by drone would increase with an increase in response time which leads to greater variability in failure probabilities. Therefore, the benefit obtained by adding robustness is greater when response times are longer. Overall, going from a single-period deterministic (SP-D) formulation to a multi-period robust (MP-R) formulation leads to an average simulated coverage improvement of 0.60 times and 0.54 times for SS1 and SS2, respectively. Figures 5 and 6 show the model solution and an MCS simulation solution (having simulated coverage close to the average value) for SP-D and MP-R, respectively, for SS2 and $q = 15$. Accommodating uncertainty in decision-making leads to the consolidation of facilities toward the central core of the Portland metropolitan area. Shorter travel distances lead to better coverage reliability in in the MP-R model.

Figure 7 shows the ratio of average simulated coverage to the model coverage (ASC-to-MC). The closer the value is to 1 the better, as it indicates that the expected

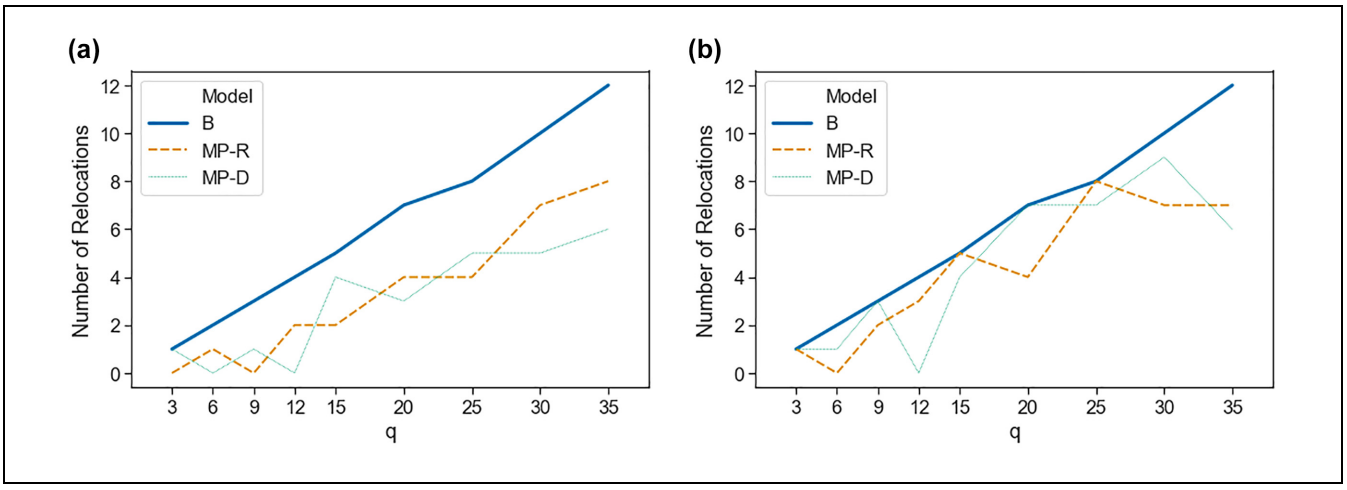


Figure 3. Facility relocations in multi-period formulation (*B* represents maximum allowable facility relocations): (*a*) SS1 and (*b*) SS2.

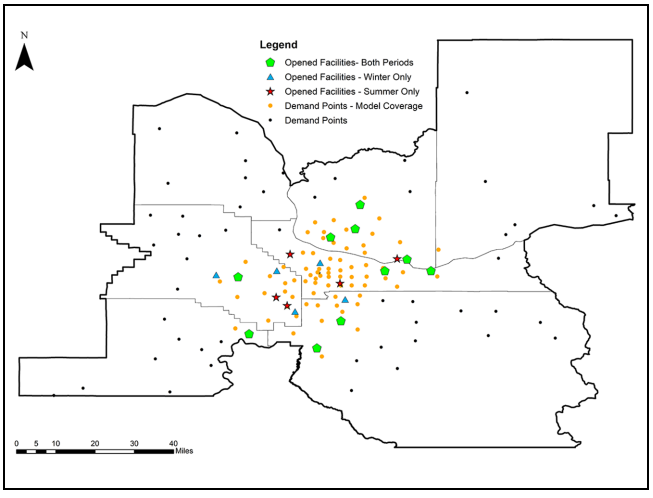


Figure 4. Facility relocation and model coverage for MP-R (SS2; $q = 15$).
Note: MP-R = multi-period robust model.

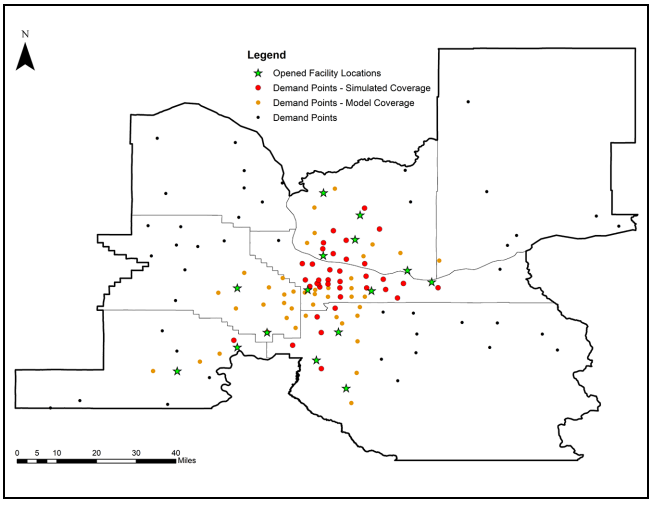


Figure 5. Opened facility locations and demand point coverage for SP-D (SS2; $q = 15$).
Note: SP-D = single-period deterministic model.

performance is close to real-life simulated scenarios. Accounting for robustness and/or extending to multi-period formulation leads to better outcomes on this metric. The ratio has a generally positive correlation with increasing values of q. This is expected, as with more opened facilities, the access to a demand point improves, and therefore, the coverage reliability also improves.

Table 3 shows the sensitivity of increasing conservatism on the coverage. For SS1, increasing robustness by increasing Γ_i^t from 1 to 2 does not change the average simulated coverage much (-0.01 times). For SS2, this results in slightly better average simulated coverage (0.04 times). Computational times on the other hand typically increased with an increase in the budget of robustness. However, all models still converged in 8 h, which is still not much considering a planning period of one year. Figure 8 shows the variation of computational times with the budget of robustness.

Significant improvements in range of variation in simulated coverage as well as in the ratio ASC-to-MC were found, especially for larger values of q. These results are, as expected, that accounting for a greater amount of uncertainty should lead to reduced model coverage (because of increased conservatism) and less variability in results (because of reduced probability of constraint violation). Therefore, finding a trade-off by changing the budget of robustness (Γ_i^t) can help to improve the simulated coverage values, and reduce the gap from the model coverage. For example, Figure 9 shows variation in model and average simulated coverage with increasing

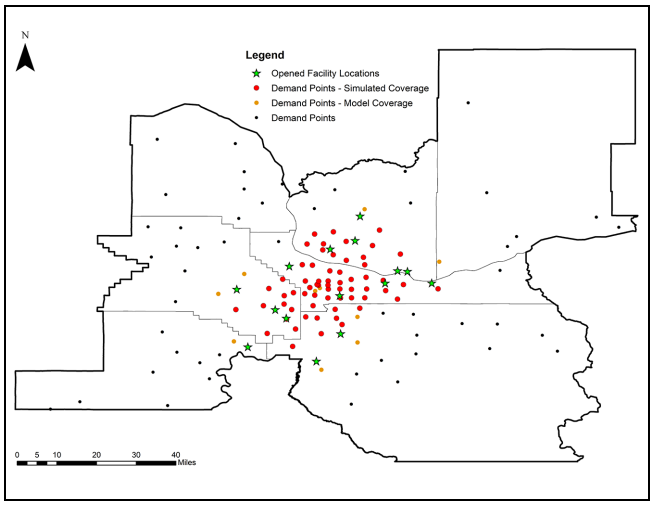


Figure 6. Opened facility locations and demand point coverage for MP-R (SS2; $q = 15$; $\Gamma_i^t = 1$).
Note: MP-R = multi-period robust mode.

value of Γ_i^t for MP-R SS1 model with $q = 35$. It can be noticed that the gap between the model and average simulated coverage is the minimum when $\Gamma_i^t = 4$.

Figure 10 shows a model solution and an MCS simulation solution (having simulated coverage close to the average value) for MP-R with $\Gamma_i^t = 2$ (SS2 and $q = 15$). Increasing conservatism further consolidates facilities around the central core compared with the case when $\Gamma_i^t = 1$ in MP-R, leading to better outcomes in simulated coverage.

Incorporating Equity in Decision Making

In the previous sections, the coverage importance was just based on the normalized population of the demand points. However, it is possible to incorporate equity-related weights to determine coverage importance. For the case study, it can be considered that the facility locations that are not opened still have a defibrillator available onsite, just that it cannot be transported. Therefore, distance to the nearest potential facility location could be considered as a metric of equity, as in Mesa et al. (*42*). The greater the minimum distance to a potential facility location from a demand point, the less equitable it is, and the more coverage importance it should get. The normalized inequity metric is calculated as:

- Distance to closest possible drone launch site from demand point i: $mindist(i)$
- Normalized inequity metric of demand point $i = \left\lceil \frac{100 \times mindist(i)}{\text{maximumvalueof}mindist(i)} \right\rceil$

For calculating the coverage importance metric, 50% weightage is assumed for both the normalized population parameter and the normalized inequity metric. Other parameters are set to their default values. The summary of results is shown in Figure 11. The simulated coverage values when equity is included are much lower than the values when equity is not included. When equity is included, the demand points far away from potential facility locations are given more importance, but most of them cannot even be accessed in the target response times (i.e., $|S_i|$ is a very small number). The spatial distribution of facilities and the demand coverage when equity is included is shown in Figure 12 for the MP-R SS2 model with $q = 15$. It can be noticed that Figures 6 and 12 are very similar, covering almost the same demand points and most facilities opened at the same spot. A primary reason for this is the distribution of facility locations and demand points. The demand points outside the more densely populated central core are located too far away

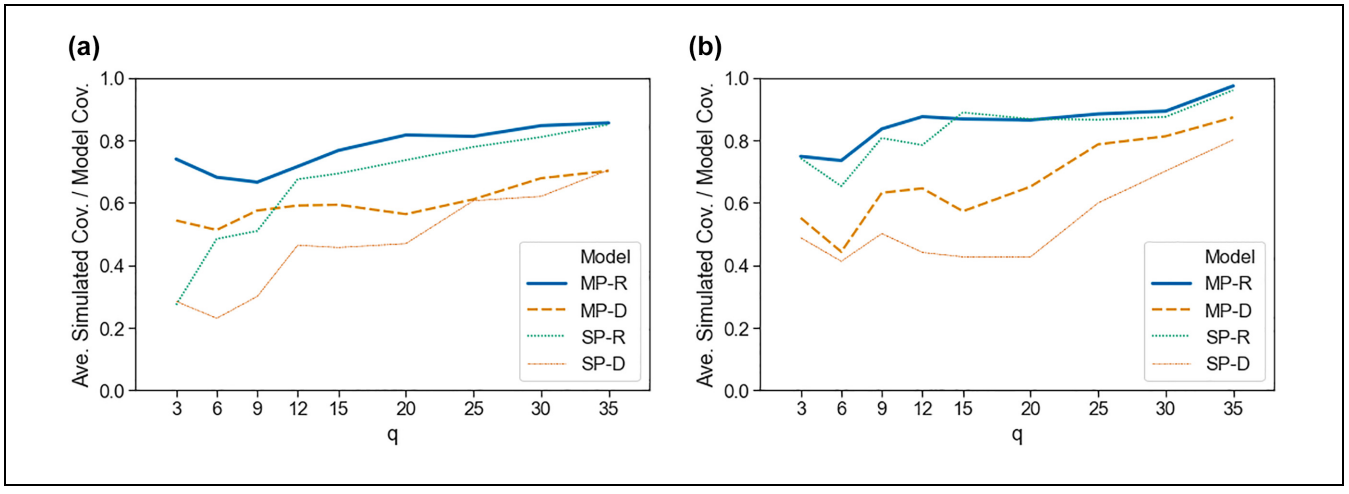


Figure 7. Ratio of average simulated coverage to model coverage: (*a*) SS1 and (*b*) SS2.

Table 3. Sensitivity to Increasing Conservatism in Decision-Making for Multi-Period Formulation

		SS1				SS2			
			Simulated coverage (%)				Simulated coverage (%)		
Γ_i^t	No. of drone launch sites, q	Model Coverage (%)	Minimum	Average	Maximum	Model Coverage (%)	Minimum	Average	Maximum
0	3	15.76	5.81	8.56	10.25	44.85	23.27	24.75	28.07
	6	27.41	7.90	14.03	19.43	69.99	14.96	31.01	45.74
	9	37.93	14.66	21.79	28.22	82.18	45.05	51.95	60.25
	12	47.02	19.22	27.83	35.43	86.23	47.44	55.65	66.15
	15	53.90	24.76	32.04	39.81	89.60	41.87	51.32	64.99
	20	62.31	25.30	35.16	44.31	93.38	50.48	60.82	71.48
	25	67.19	34.45	40.98	47.50	94.73	68.33	74.49	78.55
	30	68.36	37.22	46.33	55.69	95.23	67.04	77.36	84.77
	35	68.50	40.88	48.01	58.19	95.29	77.83	83.27	90.67
1	3	12.57	5.96	9.28	11.11	35.37	21.42	26.47	32.60
	6	24.37	13.89	16.59	19.55	62.69	36.59	46.01	56.38
	9	33.52	16.30	22.30	26.97	75.80	56.08	63.44	67.07
	12	41.90	24.52	29.96	35.67	82.60	66.18	72.25	79.38
	15	49.28	32.39	37.82	44.85	87.01	72.77	75.36	79.02
	20	55.45	35.58	45.26	53.67	90.73	72.62	78.47	85.97
	25	59.92	43.00	48.71	54.68	92.58	77.26	81.81	89.09
	30	62.28	48.99	52.58	56.05	93.21	77.98	83.21	88.86
	35	62.28	50.92	53.26	56.53	93.38	86.41	90.91	92.70
2	3	12.57	5.96	9.28	11.11	33.85	23.96	25.98	31.62
	6	22.35	8.61	15.13	20.89	59.92	41.21	48.19	55.27
	9	30.99	16.12	21.36	25.74	73.60	57.54	63.83	69.49
	12	39.18	26.88	29.39	32.48	80.51	73.48	76.81	79.35
	15	45.65	32.99	38.29	45.11	85.40	75.27	79.28	82.39
	20	52.23	39.72	46.24	52.62	89.81	81.85	85.18	87.84
	25	56.59	43.12	49.16	53.87	92.01	82.54	86.01	86.86
	30	60.07	48.72	51.70	55.13	93.00	85.04	88.45	91.00
	35	61.92	51.37	54.68	58.46	93.38	87.19	89.53	90.20

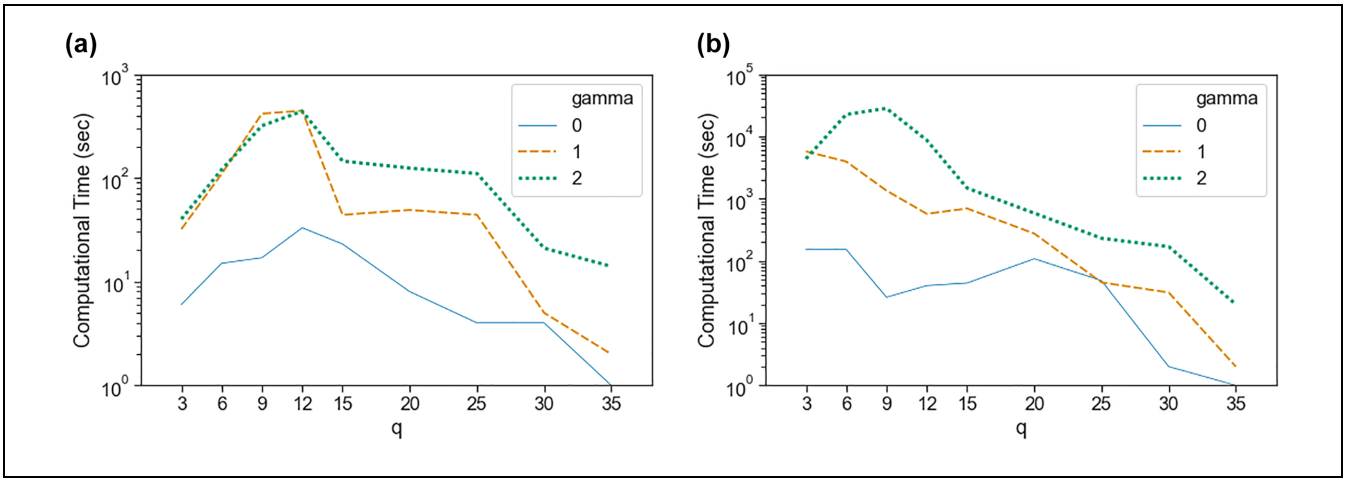


Figure 8. Computational times for varying values of Γ_i^t in multi-period formulation: (*a*) SS1 and (*b*) SS2.

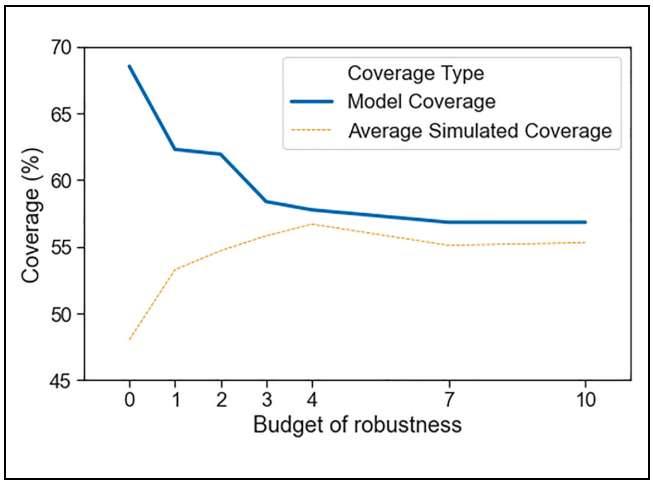


Figure 9. Model and average simulated coverage with increasing values of budget of robustness Γ_i^t (MP-R SS1 with $q = 35$).
Note: MP-R = multi-period robust model.

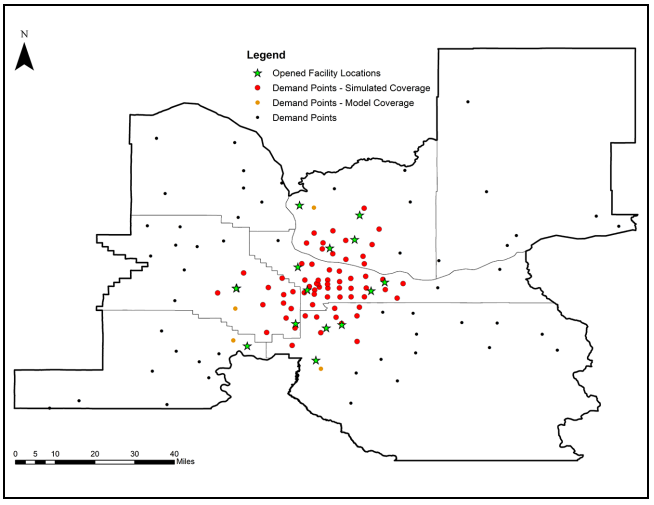


Figure 10. Opened facility locations and demand point coverage for MP-R (SS2; $q = 15$; $\Gamma_i^t = 2$).
Note: MP-R = multi-period robust model.

from the potential facility locations. For the response times used in the case study, it does not make any practical difference if equity is included or not. However, for longer response times, equity inclusion could be beneficial (longer response times lead to larger values of $|S_i|$, which make it easier to meet service reliability target for all demand points).

Aringhieri et al. (*17*) state that equity is still one of the most challenging concerns for emergency medical services. More comprehensive methodologies that explicitly address equity concerns should be explored. Previous works in facility location have addressed equity by using metrics based on distance, exclusion, and conditional value-at-risk in model formulation (*43*).

Conclusion

This paper proposes a robust multi-period maximum covering facility location problem with coverage reliability (MP-R). MP-R is a generalized variant of the robust uncertain set covering the problem proposed by Lutter et al. (*2*). The problem incorporates uncertainty in travel times via chance constraints and uses robust optimization using polyhedral uncertainty sets to tackle uncertainty.

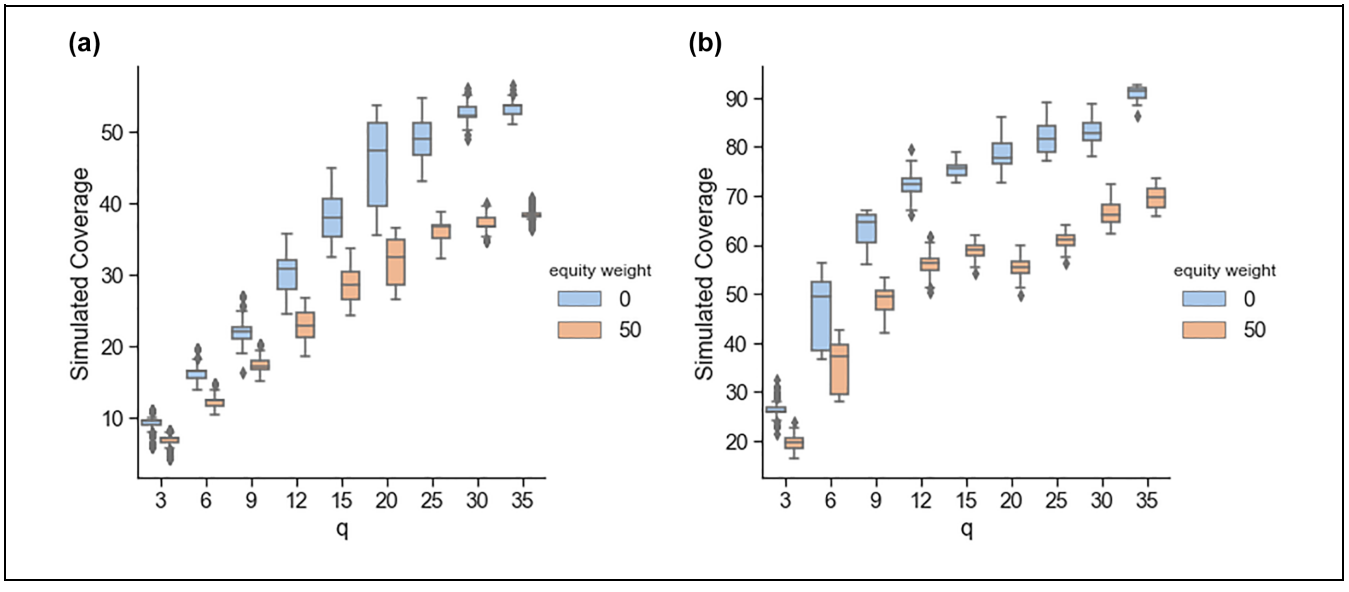


Figure 11. Effect of incorporating equity on simulated coverage: (*a*) SS1 and (*b*) SS2.

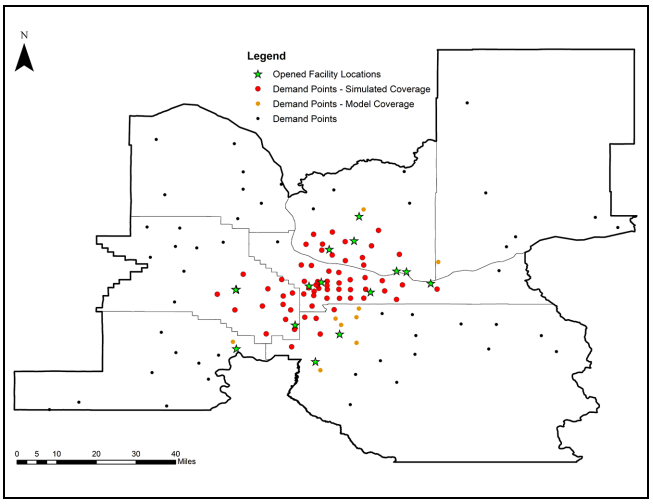


Figure 12. Opened facility locations and demand point coverage for MP-R with equity inclusion (SS2; $q = 15$; $\Gamma_i^t = 1$).
Note: MP-R = multi-period robust model.

More conservative solutions can be obtained by increasing the value of the parameters.

A case study of the use of UAVs, or drones, to deliver defibrillators in the Portland metropolitan area is proposed. The uncertainty in drone travel times is a product of natural variability in wind speeds and directions. In Portland, the wind characteristics (speed and direction) change drastically between the summer months (April to September) and winter months (October to March). Therefore, multiple periods are thought of as a discretization of recurring planning intervals (here, one whole year). The effect of extending from a single period formulation (a whole year) to a multi-period formulation (two different time periods: summer and winter) is evaluated.

The value of adding robustness and extending to a multi-period formulation was evaluated utilizing a novel Monte Carlo simulation scheme. The results highlighted that utilizing a multi-period formulation was particularly beneficial when response time thresholds were short or when uncertainty is not accounted for in the model. On the other hand, adding robustness to the deterministic models was more beneficial for single-period formulations or when response time thresholds were longer. Combining these different strengths led to an increase in average simulated coverage of MP-R by 57% compared with the deterministic single-period formulation (SP-D). Geographically, accounting for uncertainty (in MP-R) consolidates the facility locations toward the dense central core of the metro area compared with more spread out locations in SP-D. A more compact facility layout in MP-R improves the level of service in the central core of the metropolitan area, leading to superior simulated coverage.

For the MP-R model, a sensitivity analysis on the facility relocation cost budget showed very minor changes in model coverage as well as simulated coverage values. This implies that simply providing the model with more detailed information by discretizing over the planning period (even when facility relocation is not allowed) is helpful rather than providing the average information of the planning period. From the case study, when the response times are shorter, it is recommended that an existing SP-D model should be extended to MP-R (i.e., incorporating uncertainty and discretizing to multiple periods). When the response times are longer, only incorporating uncertainty in the SP-D model is sufficient and multiple periods are not necessary.

The presented formulation can be used to analyze equity gaps and the need for additional resources. Analysis of distance-based equity inclusion in the objective yielded poorer coverage values. Equity inclusion increases the coverage importance of demand points further away from potential drone launch sites, but response times used in the study were too short for these points to be covered reliably. Geographically, equity inclusion did not affect the facility locations and demand point coverage significantly. However, for longer response times than used in this study, equity inclusion could be beneficial.

Even with the MP-R model providing the best performance, a significant gap exists between model coverage and the simulated coverage values. A major contributing factor is the assumption of independence among the failure probabilities. While some of the gap can be addressed by adjusting the budget of uncertainty and increasing the number of opened facilities, there is still a need to account for correlation in failure probabilities. Additionally, the study assumed that all the accessible open facilities respond to the demand while not considering the possible unavailability of a drone at a located launch site. Future studies should also focus on including capacity considerations at located launch sites.

Author Contributions

The authors confirm contribution to the paper as follows: study conception and design: D. R. Chauhan, A. Unnikrishnan, M. A. Figliozzi, S. D. Boyles; data collection: D. R. Chauhan; analysis and interpretation of results: D. R. Chauhan, A. Unnikrishnan, M. A. Figliozzi, S. D. Boyles; draft manuscript preparation: D. R. Chauhan, A. Unnikrishnan, M. A. Figliozzi, S. D. Boyles. All authors reviewed the results and approved the final version of the manuscript.

Declaration of Conflicting Interests

The author(s) declared no potential conflicts of interest with respect to the research, authorship, and/or publication of this article.

Funding

The author(s) disclosed receipt of the following financial support for the research, authorship, and/or publication of this article: This work was partially supported by the Freight Mobility Research Institute (FMRI) and the Center for Advanced Multimodal Mobility Solutions and Education (CAMMSE) U.S. DOT University Transportation Centers (UTCs). Additionally, the authors acknowledge the support received through the National Science Foundation (NSF) under grants CMMI-1562109/1562291: Collaborative Research: Non-Additive Network Routing and Assignment Models, CMMI-1636154: Optimal Control of a Swarm of Unmanned Aerial Vehicles for Traffic Flow Monitoring in Post-disaster Conditions, and CMMI 1826320/1826337: Collaborative Research: Real-Time Stochastic Matching Models for Freight Electronic Marketplace.

ORCID iDs

Darshan Rajesh Chauhan https://orcid.org/0000-0001-5309-3130
Avinash Unnikrishnan https://orcid.org/0000-0001-6737-0485
Miguel A. Figliozzi https://orcid.org/0000-0003-2120-4929

Data Accessibility Statement

The data presented in the paper are available freely at https://github.com/drc1807/RMP-MCFLP-CR.

References

1. National Fire Protection Association. *NFPA 1710: Standard for the Organization and Deployment of Fire Suppression Operations, Emergency Medical Operations, and Special Operations to the Public by Career Fire Departments*. National Fire Protection Association, Quincy, MA, 2020.
2. Lutter, P., D. Degel, C. Büsing, A. M. Koster, and B. Werners. Improved Handling of Uncertainty and Robustness in Set Covering Problems. *European Journal of Operational Research*, Vol. 263, No. 1, 2017, pp. 35–49. https://doi.org/10.1016/j.ejor.2017.04.044.
3. Budge, S., A. Ingolfsson, and D. Zerom. Empirical Analysis of Ambulance Travel Times: The Case of Calgary Emergency Medical Services. *Management Science*, Vol. 56, No. 4, 2010, pp. 716–723. https://doi.org/10.1287/mnsc.1090.1142.
4. Ayamga, M., S. Akaba, and A. A. Nyaaba. Multifaceted Applicability of Drones: A Review. *Technological Forecasting and Social Change*, Vol. 167, 2021, p. 120677. https://doi.org/10.1016/j.techfore.2021.120677.
5. Nyaaba, A. A., and M. Ayamga. Intricacies of Medical Drones in Healthcare Delivery: Implications for Africa. *Technology in Society*, Vol. 66, 2021, p. 101624. https://doi.org/10.1016/j.techsoc.2021.101624.
6. Leonard, M. Amazon Prime Air Gets FAA Clearance for Drone Delivery on "Highly Rural" Test Range, September 1, 2020. https://www.supplychaindive.com/news/amazon-prime-air-faa-clearance-drone-delivery-rural-test-range/584436/. Accessed February 14, 2022.
7. FAA. Unmanned Aircraft Systems (UAS) BEYOND, 2021. https://www.faa.gov/uas/programs_partnerships/beyond/. Accessed February 2, 2022.
8. Glick, T. B., M. A. Figliozzi, and A. Unnikrishnan. Case Study of Drone Delivery Reliability for Time-Sensitive Medical Supplies With Stochastic Demand and Meteorological Conditions. *Transportation Research Record: Journal of the Transportation Research Board*, 2022. 2676: 242–255.
9. Bertsimas, D., and M. Sim. The Price of Robustness. *Operations Research*, Vol. 52, No. 1, 2004, pp. 35–53. https://doi.org/10.1287/opre.1030.0065.
10. Schmid, V., and K. F. Doerner. Ambulance Location and Relocation Problems With Time-Dependent Travel Times. *European Journal of Operational Research*, Vol. 207, No. 3, 2010, pp. 1293–1303. https://doi.org/10.1016/j.ejor.2010.06.033.
11. Erdoğan, G., E. Erkut, A. Ingolfsson, and G. Laporte. Scheduling Ambulance Crews for Maximum Coverage. *Journal of the Operational Research Society*, Vol. 61, No. 4, 2010, pp. 543–550. https://doi.org/10.1057/jors.2008.163.
12. Azizan, M. H., C. S. Lim, W. L. W. Hatta, and L. C. Gan. Application of Openstreetmap Data in Ambulance Location Problem. *Proc., 2012 Fourth International Conference on Computational Intelligence, Communication Systems and Networks*, Phuket, Thailand. IEEE, New York, NY, 2012, pp. 321–325. https://doi.org/10.1109/CICSyN.2012.66.
13. Enayati, S., M. E. Mayorga, H. K. Rajagopalan, and C. Saydam. Real-Time Ambulance Redeployment Approach to Improve Service Coverage With Fair and Restricted Workload for EMS Providers. *Omega*, Vol. 79, 2018, pp. 67–80. https://doi.org/10.1016/j.omega.2017.08.001.
14. Erkut, E., A. Ingolfsson, and G. Erdoğan. Ambulance Location for Maximum Survival. *Naval Research Logistics (NRL)*, Vol. 55, No. 1, 2008, pp. 42–58. https://doi.org/10.1002/nav.20267.
15. Zaffar, M. A., H. K. Rajagopalan, C. Saydam, M. Mayorga, and E. Sharer. Coverage, Survivability or Response Time: A Comparative Study of Performance Statistics Used in Ambulance Location Models via Simulation–Optimization. *Operations Research for Health Care*, Vol. 11, 2016, pp. 1–12. https://doi.org/10.1016/j.orhc.2016.08.001.
16. Naoum-Sawaya, J., and S. Elhedhli. A Stochastic Optimization Model for Real-Time Ambulance Redeployment. *Computers & Operations Research*, Vol. 40, No. 8, 2013, pp. 1972–1978. https://doi.org/10.1016/j.cor.2013.02.006.
17. Aringhieri, R., M. E. Bruni, S. Khodaparasti, and J. T. van Essen. Emergency Medical Services and Beyond: Addressing New Challenges Through a Wide Literature Review. *Computers & Operations Research*, Vol. 78, 2017, pp. 349–368. https://doi.org/10.1016/j.cor.2016.09.016.
18. Başar, A., B. Çatay, and T. Ünlüyurt. A Taxonomy for Emergency Service Station Location Problem. *Optimization Letters*, Vol. 6, No. 6, 2012, pp. 1147–1160. https://doi.org/10.1007/s11590-011-0376-1.
19. Li, X., Z. Zhao, X. Zhu, and T. Wyatt. Covering Models and Optimization Techniques for Emergency Response

Facility Location and Planning: A Review. *Mathematical Methods of Operations Research*, Vol. 74, No. 3, 2011, pp. 281–310. https://doi.org/10.1007/s00186-011-0363-4.
20. Pulver, A., R. Wei, and C. Mann. Locating AED Enabled Medical Drones to Enhance Cardiac Arrest Response Times. *Prehospital Emergency Care*, Vol. 20, No. 3, 2016, pp. 378–389. https://doi.org/10.3109/10903127.2015.1115932.
21. Pulver, A., and R. Wei. Optimizing the Spatial Location of Medical Drones. *Applied Geography*, Vol. 90, 2018, pp. 9–16. https://doi.org/10.1016/j.apgeog.2017.11.009.
22. Chauhan, D., A. Unnikrishnan, and M. Figliozzi. Maximum Coverage Capacitated Facility Location Problem With Range Constrained Drones. *Transportation Research Part C: Emerging Technologies*, Vol. 99, 2019, pp. 1–18. https://doi.org/10.1016/j.trc.2018.12.001.
23. Chauhan, D. R., A. Unnikrishnan, M. Figliozzi, and S. D. Boyles. Robust Maximum Coverage Facility Location Problem With Drones Considering Uncertainties in Battery Availability and Consumption. *Transportation Research Record: Journal of the Transportation Research Board*, 2021. 2675: 25–39.
24. Garner, A. A., and P. L. van den Berg. Locating Helicopter Emergency Medical Service Bases to Optimise Population Coverage Versus Average Response Time. *BMC Emergency Medicine*, Vol. 17, No. 1, 2017, p. 31. https://doi.org/10.1186/s12873-017-0142-5.
25. Røislien, J., P. L. van den Berg, T. Lindner, E. Zakariassen, K. Aardal, and J. T. van Essen. Exploring Optimal Air Ambulance Base Locations in Norway Using Advanced Mathematical Modelling. *Injury Prevention*, Vol. 23, No. 1, 2017, pp. 10–15. https://doi.org/10.1136/injuryprev-2016-041973.
26. Ballou, R. H. Dynamic Warehouse Location Analysis. *Journal of Marketing Research*, Vol. 5, No. 3, 1968, pp. 271–276. https://doi.org/10.1177/002224376800500304.
27. Nickel, S., and F. Saldanha da Gama. Multi-Period Facility Location. In *Location Science* (Laporte, G., S. Nickel, and F. Saldanha da Gama, eds.), Springer, Cham, 2019, pp. 303–326. https://doi.org/10.1007/978-3-030-32177-2_11.
28. Vatsa, A. K., and S. Jayaswal. Capacitated Multi-Period Maximal Covering Location Problem With Server Uncertainty. *European Journal of Operational Research*, Vol. 289, No. 3, 2021, pp. 1107–1126. https://doi.org/10.1016/j.ejor.2020.07.061.
29. Kim, D., K. Lee, and I. Moon. Stochastic Facility Location Model for Drones Considering Uncertain Flight Distance. *Annals of Operations Research*, Vol. 283, No. 1, 2019, pp. 1283–1302. https://doi.org/10.1007/s10479-018-3114-6.
30. Ghelichi, Z., M. Gentili, and P. B. Mirchandani. Logistics for a Fleet of Drones for Medical Item Delivery: A Case Study for Louisville, KY. *Computers & Operations Research*, Vol. 135, 2021, p. 105443. https://doi.org/10.1016/j.cor.2021.105443.
31. Ben-Tal, A., L. El Ghaoui, and A. Nemirovski. *Robust Optimization*. Princeton University Press, Princeton, NJ, 2009. https://doi.org/10.1515/9781400831050.
32. Bertsimas, D., D. B. Brown, and C. Caramanis. Theory and Applications of Robust Optimization. *SIAM Review*, Vol. 53, No. 3, 2011, pp. 464–501. https://doi.org/10.1137/080734510.
33. Gabrel, V., C. Murat, and A. Thiele. Recent Advances in Robust Optimization: An Overview. *European Journal of Operational Research*, Vol. 235, No. 3, 2014, pp. 471–483. https://doi.org/10.1016/j.ejor.2013.09.036.
34. Gorissen, B. L., İ. Yankoğlu, and D. den Hertog. A Practical Guide to Robust Optimization. *Omega*, Vol. 53, 2015, pp. 124–137. https://doi.org/10.1016/j.omega.2014.12.006.
35. Goh, J., and M. Sim. Distributionally Robust Optimization and Its Tractable Approximations. *Operations Research*, Vol. 58, No. 4 part 1, 2010, pp. 902–917. https://doi.org/10.1287/opre.1090.0795.
36. Delage, E., and Y. Ye. Distributionally Robust Optimization Under Moment Uncertainty With Application to Data-Driven Problems. *Operations Research*, Vol. 58, No. 3, 2010, pp. 595–612. https://doi.org/10.1287/opre.1090.0741.
37. Ben-Tal, A., and A. Nemirovski. Robust Solutions of Uncertain Linear Programs. *Operations Research Letters*, Vol. 25, No. 1, 1999, pp. 1–13. https://doi.org/10.1016/S0167-6377(99)00016-4.
38. Philips. Side by Side. Step by Step. Philips HeartStart OnSite AED, 2022. https://www.documents.philips.com/assets/20170523/5777e26b79a1438b8138a77c014ef7d9.pdf. Accessed February 14, 2022.
39. Figliozzi, M. A. Lifecycle Modeling and Assessment of Unmanned Aerial Vehicles (Drones) CO_2e Emissions. *Transportation Research Part D: Transport and Environment*, Vol. 57, 2017, pp. 251–261. https://doi.org/10.1016/j.trd.2017.09.011.
40. Census-Bureau, U. S. And American-FactFinder. 2017 American Community Survey 5-Year Estimates, 2018. https://data.census.gov/cedsci/. Accessed March 8, 2020.
41. Gurobi Optimization, L. *Gurobi Optimizer Reference Manual*, 2020. http://www.gurobi.com.
42. Mesa, J. A., J. Puerto, and A. Tamir. Improved Algorithms for Several Network Location Problems With Equality Measures. *Discrete Applied Mathematics*, Vol. 130, No. 3, 2003, pp. 437–448. https://doi.org/10.1016/S0166-218X(02)00599-1.
43. Sirupa, R. *Incorporating Conditional β-Mean Based Equity Metric in Coverage Based Facility Location Problems*. Master's thesis. Portland State University, 2021. https://doi.org/10.15760/etd.7587.